HIGH POWER FAULT TOLERANT MOTORS FOR AEROSPACE APPLICATIONS

G.J.Atkinson, B.C.Mecrow. Newcastle University

I. INTRODUCTION

An aircraft main engine fuel pump is coupled directly to the main engine drive shaft via a gear box. As such the pump's speed is proportional to the engine speed.

An aircraft requires the most fuel at take off. This is when the engine is running at its slowest due to the dense atmosphere at ground level.

In the thin atmosphere at altitude, the engine runs faster, and via the gear box the fuel pump runs faster, delivering more fuel. However less fuel is required than at take off. The excess fuel is diverted back to the fuel tank, an inefficient, but reliable arrangement.

Much work is being done in the aerospace industry to convert the various aircraft mechanical, hydraulic and pneumatic power systems to one globally optimised electrical system.

The main engine gear box that drives the pump can be replaced with an electric motor and drive. The drive, linked to an engine management system, can control the speed of the fuel pump to deliver the correct amount of fuel required during the various stages of the flight cycle.

A 16kW 15,000 revs/min fault tolerant electric fuel pump drive was developed, built and tested [1]. The stator consists of four isolated phases which give electrical, thermal and magnetic isolation. The one-per-unit inductance limits a phase short circuit to the rated current. Fuel flows through the air-gap and slots providing an efficient coolant, this allows the machine to operate with a high electrical loading. A six pole samarium cobalt permanent magnet rotor gives the machine a high magnetic loading.

The fault tolerant drive was tested whilst mated to its fuel pump and aviation fuel was successfully pumped under normal and faulted conditions with the machine running at 16kW and 15,000 revs/min.

II. HIGH POWER FAULT TOLERANT MOTOR

Following the successful testing of the 16kW electric fuel pump drive, The Goodrich Corporation identified a need for a 100kW drive capable of powering a typical medium to large passenger aircraft fuel pump. As with the previous lower power demonstrators, the drive must be fault tolerant. Four phases were chosen as being a good compromise between the overrating factor and drive reliability.

Initial designs were based around a re-scaled version of the 16kW machine and analysis showed a significant decrease in efficiency, with full load losses exceeding 20kW. An investigative design process considered the individual loss components and then combined the findings to produce an optimum 100kW fault tolerant machine design.

Rotor eddy current loss

Fault tolerance requires isolated phases. This results in a rich harmonic spectrum of the air-gap magnetic field, to which the electrically conducting magnets and sleeve are exposed. Consequently rotor eddy current loss due to the asynchronous harmonics is significant [2], exceeding 8kW in the initial design. The majority of rotor loss is due to the 5^{th} air-gap harmonic, by altering the stator design the 5^{th} harmonic is reduced whilst maximising the torque producing 3^{rd}. Not only is rotor eddy current loss reduced by 27%, but the maximised 3^{rd} harmonic allows for a reduction in the electrical loading, thereby reducing winding and stator losses.

Winding loss

Increased speed for the same EMF as the 16kW machine has resulted in less turns per phase. With a larger current there are less, but larger diameter conductors. Skin and proximity effects become significant, for a solid conductor, AC winding loss at 1.5kHz is 5.4 times DC winding loss.

The one per unit inductance, required to limit the machine's short circuit current, depends on a

large cross slot leakage flux. This is imposed on the conductors in the vicinity, further exacerbating the AC effects. The conductor marked X, Figure 1, experiences AC loss equal to 20 times the DC loss.

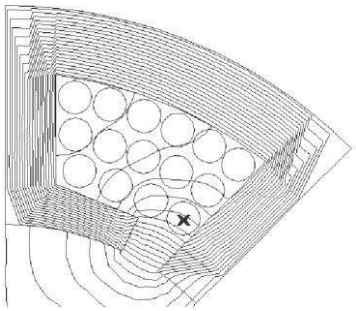

Figure 1. Energised slot flux plot.

The use of multi-strand conductors plus careful positioning of the coils bring the AC winding close to the DC loss value.

Iron loss

Aerospace grade cobalt steel laminations ensure low stator losses. Whilst thinner laminations will further reduce iron loss, this is only 7% of total loss and it was felt that the additional work and cost associated with more and thinner laminations was not justified. Therefore 0.35mm Rotelloy laminations have been used.

Viscous drag loss

The high loading of this machine is only possible with fuel as a cooling. Fuel in contact with the rotating rotor presents a drag force. At high speeds this may be in excess of 20% of the machine output.

Viscous drag is proportional to the rotor radius to the power 3.8. The large magnets allow for a large magnetic gap, this is obtained through a reduction in rotor radius for the same stator bore. The reduction in rotor drag loss comes at the cost of reduced stator-rotor coupling, and consequently an increased electrical load and associated losses for the same torque. A 6mm magnetic gap offers the best compromise.

III. THE 100KW 30,000RPM FAULT TOLERANT MACHINE

A 100kW, 30000rpm fault tolerant motor has been designed and constructed. The stator has a 60° wound tooth span and smaller spacer teeth to magnetically, thermally and electrically isolate the phases, Figure 2. 256 strand Litz wire is used to minimise AC effects at the 1.5kHz power frequency.

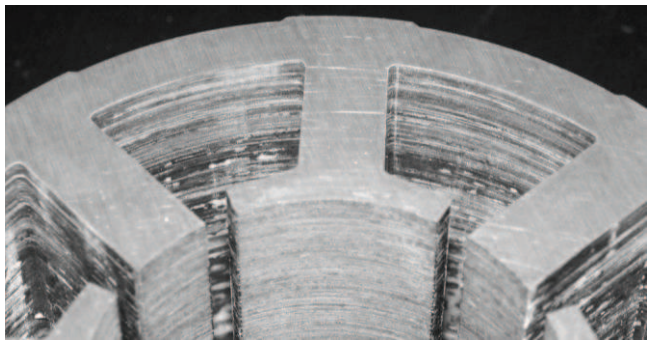

Figure 2. 100kW stator.

The permanent magnet rotor is constructed from Samarium Cobalt magnets retained by an Inconel sleeve. The magnets are arranged in a Halbach array to provide a high air-gap flux density. Fuel cooling allows for a high electrical loading and consequently the 100kW rotor is only 73mm in diameter with an active length of 81mm, Figure 3.

Figure 3. The 100kW permanent magnet rotor.

The 100kw machine is mounted on a high speed no-load test rig, Figure 4. A DC machine is used to back drive the fault tolerant motor to 26,000 rpm. Mechanical power input is measured using a torque transducer and several internal temperature measurements are monitored.

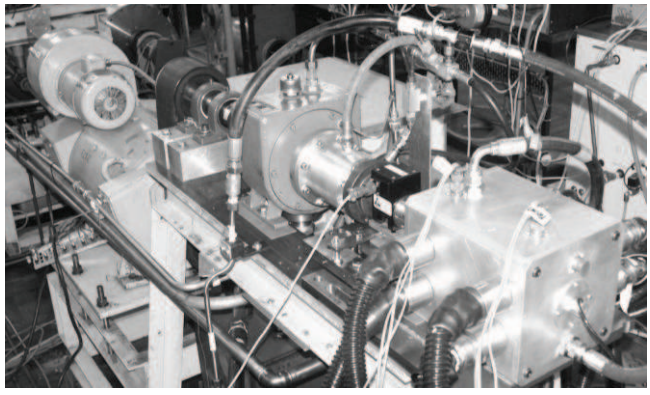

Figure 4. The high speed no-load test rig.

IV. INITIAL TEST RESULTS

Electromagnetic characteristics, thermal characteristics and efficiency have all been assessed using the high speed no-load test rig and a series of static tests. Full load, full speed performance is inferred from these results.

The back EMF, Figure 5, is a good quality sinusoid with minimal harmonics, as expected from a Halbach array.

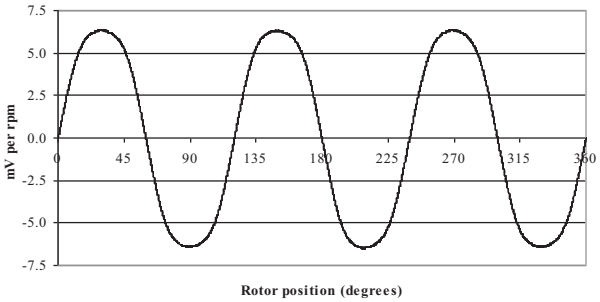

Figure 5. Back EMF profile.

Static torque has been measured up to 49% of the full load current and interpolation suggests a full load torque of 30.7Nm. Figure 6 is the static torque curve for a full revolution minus cogging.

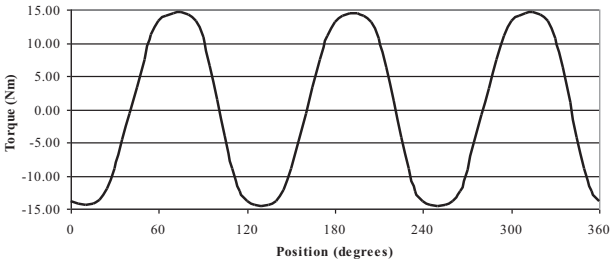

Figure 6. Static torque against position minus cogging.

Fault tolerance depends on minimal electrical, thermal and magnetic coupling between phases. As shown in Table 1, there is only 5% mutual coupling between adjacent phases. Thermal coupling between phases is also negligible.

Table 1. Self and mutual inductance

Self inductance	151 μH
Mutual (adjacent)	8.6 μH
Mutual (Opposite)	2.2 μH

Fault tolerance also depends upon the ability to withstand a phase short circuit. The short circuit current will develop to a magnitude sufficient to provide MMF capable of fully rejecting the permanent magnet flux, as shown in Figure 7. A single phase was shorted whilst the machine was driven, and once fully developed the short circuit current is 102Arms. This is less than the machine's rated current.

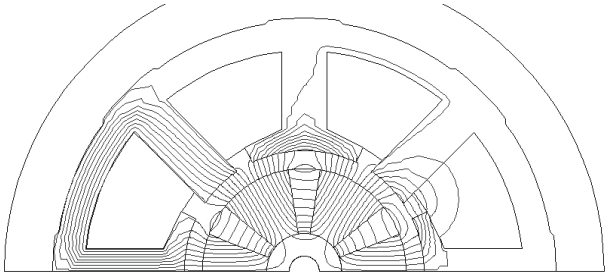

Figure 7. Short circuit flux plot.

The benefit of oil cooling can be seen when energising a phase and measuring the peak temperature rise whilst naturally cooled in air and then cooled by an oil flow. As shown in Figure 8, a 100A load results in a temperature rise of 121ºC in air, compared to only 28ºC in a modest flow Fusus oil. (Fusus was used as an alternative to aviation fuel in the University laboratory)

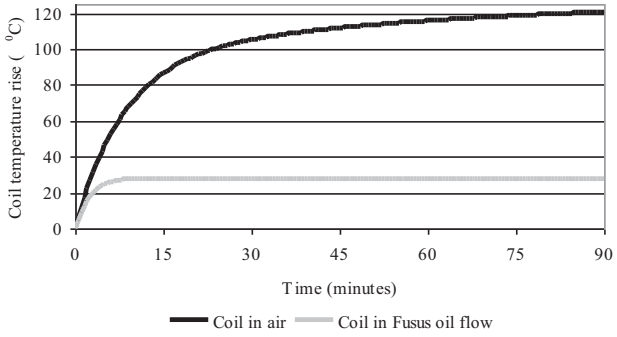

Figure 8. Temperature rise of a loaded coil in air and in flowinf oil.

No load loss is the sum of iron loss, drag loss and bearing loss. This has been measured directly using the torque transducer whilst driving the fault tolerant machine with the DC machine.

Initial tests indicated no-load losses were 70% greater than expected, however further inspection showed a large variation in the measurement over time. Analysis of the test data highlights the strong dependency on the oil temperature. As the oil heats the viscosity reduces, and with it the viscous drag. No-load loss at 15,000rpm was found to fall from 4kW to 1.5kW as the oil approached 70°C.

An aluminium dummy rotor was used to further separate the no-load losses. In the absence of permanent magnets no-load loss is bearing loss (a negligible value) plus viscous drag loss. At 26,000rpm viscous drag loss was measured as 4.9kW in Fusus. This projects to around 5kW in aviation fuel at 30,000rpm. As shown in Figure 9

the measured results are considerably less than the predictions using empirical formulae [3].

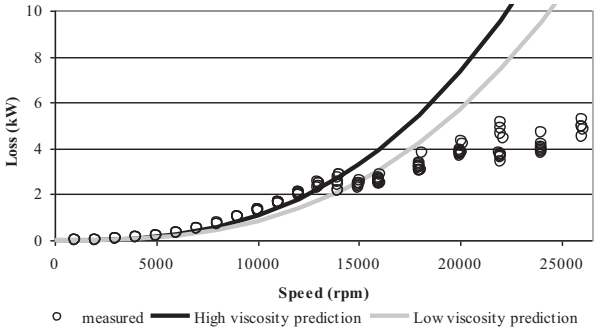

Figure 9. Predicted and measured drag loss.

Subtraction of the dummy rotor no-load loss curve from the magnet rotor no-load loss curve should yield the iron loss curve, however, the standard deviation in the measurements is in the order of the iron loss predictions, hence this figure cannot be relied upon.

The load dependant losses are winding loss, load dependant iron loss and rotor eddy current loss. Full load loss measurements are not possible with the current test facilities; however, they can be inferred from a series dynamic and lower load static tests.

With the rotor removed a 1.5kHz current was applied to two opposing phases and actual power loss measured using a wideband power analyser. Measured loss is two phase AC winding loss + iron loss in the energised portion of the stator. Repeating this procedure with the rotor in place and locked in position, measured loss is AC winding loss + local iron loss + static rotor eddy current loss. The subtraction of the "without rotor" loss from the "with rotor" loss isolates the rotor eddy current loss.

Rotor loss was calculated using a harmonic method applied to a 2DFE model. The two diametrically opposing energised phases give an air-gap tangential magnetic field which is stationary in space and pulsating at 1.5kHz. This has been decomposed to a set of fixed magnitude, counter rotating harmonics, as shown in Figure 10. Each harmonic is applied to a finite element model of the rotor and eddy current loss calculated. As shown in Figure 11 the measured and predicted results closely agree.

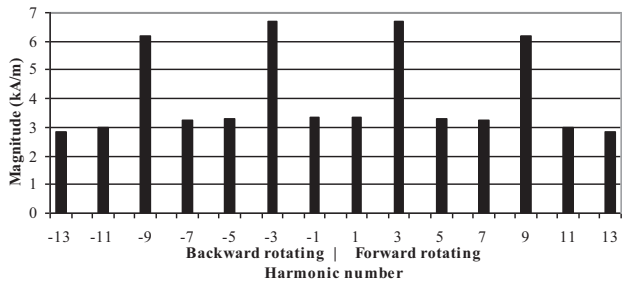

Figure 10. Air-gap harmonic spectrum during the static rotor tests.

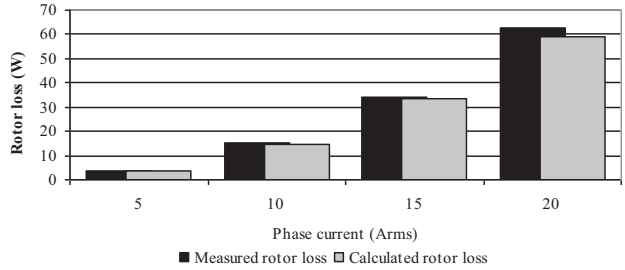

Figure 11. Measured and predicted rotor loss.

From this set of results full-load, full speed performance can be inferred and the motor is expected to operate at 100kW, 30,000rpm with an efficiency of 84.5%.

V. CONCLUSION

A 100kW, 30,000rpm fault tolerant permanent magnet motor has been designed, constructed and tested. The design takes advantage of the fuel cooling to deliver a fault tolerant machine with a high power density, essential for an aerospace application.

Full load and full speed performance is inferred from a series of tests using the high speed no-load test rig and static tests. It is expected that the motor will deliver 100kW at 30,000rpm with an efficiency of 84.5% in aviation fuel. Not taking drag loss into account, the motor efficiency is above 90%.

Work is currently being carried out on the development of the 100kW controller and power system. Along with this a high power test rig is being installed and full speed, full load testing is expected in the coming year.

VI. REFERENCES

[1] Mecrow, B.C., Jack, A.J., Atkinson, D.J., Green, S., Atkinson, G.J., King, A., Green, B. 'Design and Testing of a 4 Phase Fault tolerant Permanent Magnet Machine for an Engine Fuel Pump' IEE International Electrical Machines and Drives conference, 2003.

[2] Toda, H. Xia, Z. Wang, J. Atallah, K. Howe, D. "Rotor eddy-current loss in permanent magnet brushless machines" IEEE Transactions on Magnetics, Vol. 40, No. 4, July 2004, pp.2104-2106.

[3] Bilgen, E. Boulos, R. "Functional Dependence of Torque Coefficient of Coaxial Cylinders on Gap Width and Reynolds Numbers" Transactions of the ASME,. March 1973, pp. 122-124